

Seismic performance evaluation of a ductile R/C structure with masonry infills

Abstract

The seismic performance of a ductile four-storey R/C structure with masonry infills was analyzed through nonlinear static and dynamic analyses and the effects of infills on the structural response were investigated. On the basis of results obtained from experimental tests carried out at the JRC Elsa Laboratory, numerical models were developed in order to properly simulate the seismic response of the R/C structure. A simplified approach based on nonlinear static analyses was applied for the seismic performance assessment of the R/C structure, comparing deformation capacity and demand. The expected contribution of masonry infills in terms of both strength and stiffness was evident when comparing the response of the different structural configurations under nonlinear static analyses. The increase of stiffness provided by the masonry infills led to anticipate, in terms of drift, the attainment of the different Limit States in the infilled structure compared to the bare counterpart. The presence of uniformly distributed infills considerably changed the distribution of damage throughout the structure. The maximum drift demand on the bare structure was registered at the second storey. On the contrary, the drift demand on the uniformly infilled structure concentrated at the first storey without excessive demands at the upper storeys. The influence of uniformly distributed infills on the seismic response of the investigated structure was beneficial according to the simplified assessment procedure. The effects of masonry openings on the structural response were investigated and different types of infills were considered in the numerical analyses. The presence of openings and the mechanical properties of the infills significantly affected the seismic response of the structure. The sudden drop of strength due to the failure of the infills led to damage concentration at the first storey in case of strong infills for severe seismic input motions.

Keywords: seismic response, masonry infill, opening, numerical model, nonlinear static analyses.

1. Introduction

Experience from earthquakes and experimental tests shows that infill panels, usually considered as non-structural elements, can strongly affect the global seismic response of R/C frame structures. The main purpose of this study is to evaluate the effects of masonry infills on the seismic performance of ductile R/C structures. The influence of the presence of masonry openings was analyzed and the effects of the mechanical properties of uniformly distributed masonry infills were investigated. Simplified procedures based on nonlinear static analyses were used for the seismic assessment of infilled R/C structures. Based on results of experimental tests carried out at the JRC Elsa Laboratory, Negro (1994), numerical models were developed in order to properly simulate the seismic response of a four-storey R/C structure designed for earthquake loads. Numerical results from nonlinear pushover and time-history analyses are presented for different structure configurations: a) bare structure (no infills); b) fully infilled structure (without openings); c) partially infilled structure (with openings). Two variants of masonry infills were investigated, aimed at simulating weak and strong infill panels. Autoclaved aerated concrete (AAC) infill walls were also considered in the numerical analyses.

2. Test structure and numerical models

This study was based on results of laboratory tests carried out at the JRC ELSA Laboratory at Ispra and the accuracy of the developed numerical models of bare and infilled R/C structures was evaluated through comparison with the experimental tests. The test building was designed as a high ductility R/C framed structure, according to the then current drafts of Eurocode 2 and Eurocode 8, for a peak ground acceleration of 0.3g and medium soil conditions. Figure 1 shows the plan and elevation view of the test structure. Dimensions in plan were 10 m x 10 m, the inter-storey height of the ground floor level was 3.5 m and the other inter-storey heights were 3 m. Further details concerning the test structure, the mechanical characteristics of the materials and the amount of reinforcement were reported in Negro (1994). The pseudo-dynamic tests were conducted by using an artificially generated earthquake derived from the 1976 Friuli earthquake. On the bare structure a high-level test with nominal acceleration 50% larger than the value adopted in design was preceded by a low-level test with an intensity scaling factor of 0.4. A second experimental programme was carried out to study the influence of masonry infill panels on the global behaviour of the structure. Two pseudo-dynamic tests were conducted with different infill patterns. A test was performed by infilling the two external frames with hollow brick masonry in all four stories (uniform infill distribution). The test was then repeated on the structure without infills at the first storey to create a soft-storey effect. A general view of the test building with masonry infills on the external frames is shown in Figure 1. In this study the results of numerical investigations carried out on the R/C structure were presented and the performances of the building with different infills were compared.

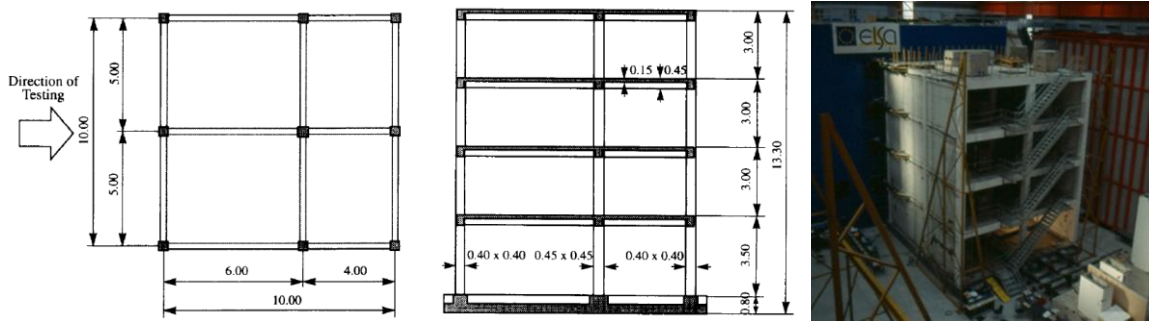


Figure 1. Plan and elevation view of the bare and infilled R/C structure

Numerical models of the R/C structure were developed by using all the available theoretical and experimental data and by comparing the numerical predictions to test results in terms of displacement and base shear time history in order to achieve appropriate values for relevant parameters. The bare and infilled structures were modelled using the computer codes Seismostruct and Ruaumoko.

In Seismostruct code the spread of inelasticity along the member length and within the member cross-section was modelled by means of a fibre modelling approach. The sectional stress-strain state of inelastic frame elements was obtained through the integration of the nonlinear uniaxial stress-strain response of the individual fibres into which the section was subdivided. Concrete was modelled by using a uniaxial constant-confinement model based on the constitutive relationship proposed by Mander et al. (1988), and later modified by Martinez-Rueda and Elnashai (1997) to cope with some problems concerning numerical stability under large displacements. The confinement effects, provided by the transverse reinforcement, were taken care of as proposed by Mander, whereby a constant confining pressure was assumed in the entire stress-strain range. The model required the introduction of 4 parameters: the compressive and tensile strengths of the unconfined concrete, the crushing strain and the confinement factor, defined as the ratio between the confined and unconfined compressive stress of the concrete. The longitudinal reinforcement was modelled through the Menegotto–Pinto model (Menegotto and Pinto, 1973). The four-node masonry panel elements were used to represent the behaviour of infill panels in the frame. Each panel is represented by five strut members, two parallel struts in each diagonal direction and a single strut acting across two opposite diagonal corners to carry the shear from the top to the bottom of the panel. The four struts use the masonry strut hysteresis model, developed by Crisafulli (2000), while the shear strut uses a bilinear hysteresis rule. The actual materials properties measured during the tests were introduced into the numerical models.

The finite element code Ruaumoko, (Carr, 2006), based on a lumped plasticity approach, was used to perform nonlinear dynamic analyses and to compute damage indices. Beams and columns were modelled using one-dimensional elastic elements with inelastic behaviour concentrated at the edges in plastic hinge regions (Giberson model) and defined by appropriate moment-curvature hysteresis rules available in Ruaumoko. The expression given in Paulay and Priestley (1992) was used for the definition of the plastic hinge length:

$$L_p = 0.08 \cdot L + (\xi \cdot f_y \cdot \phi_{\max}) \quad (1)$$

The Modified Takeda hysteresis model (Otani, 1974), widely used for reinforced concrete sections, was used to represent the moment-curvature behaviour in the hinge region of the member. The elastic

stiffness of the elements was computed according to the cracked section approach. The Takeda with slip hysteresis was used to model the behaviour of beams to take into account the effect of the slippage of the reinforcing bars. Bending moment-axial force interaction diagrams were used to account for the variation of moment capacity due to axial force. Strength degradation curve was associated to the selected hysteresis behaviour to represent possible strength reduction due to number of cycles and ductility demand. The infill panels were modelled using the equivalent diagonal strut model. Simple modelling with equivalent diagonal struts is able to simulate the global seismic response of infilled structures and is suitable for practical applications. The cyclic behaviour of the infill panel was modelled adopting the hysteresis rule proposed by Crisafulli (1997) to simulate the axial response of masonry.

The effect of the openings was taken into account by reducing the strut area and thus the infill panel stiffness. Several researchers suggest different reduction factors to describe the decrease of stiffness, depending on the dimensions and the position of the openings. In this study different stiffness reduction factors for different opening percentages were considered, Asteris (2003).

3. Validation and damage distribution

For the validation of the numerical models, nonlinear dynamic analyses were performed on the four-storey R/C structure in the different configurations assuming the same accelerogram used for the low-level and high-level pseudo-dynamic tests. First, analyses were performed on the bare structure; then, the same input motion was applied to the structure with uniform configuration of infills. The comparison of numerical predictions with experimental test results allowed to calibrate some model parameters which cannot be completely derived from theoretical considerations.

In Figure 2 the top displacement and base shear time histories derived from the pseudo-dynamic tests on the bare building were compared to the results obtained from numerical analyses performed under low-level earthquake using the developed numerical models. A very good fitting can be noted in terms of time history trend, phase and maximum values. Figure 3 shows the comparison between experimental and numerical results of the top displacement time history for the bare and uniformly infilled structures under high-level earthquake. The numerical models were able to satisfactorily reproduce the experimental results for both the structural configurations.

Numerical analyses carried out in order to compare numerical versus experimental results allowed to study the sensitivity of the structural response to some variables. They showed that the parameters governing the nonlinear behaviour of the beam affect the response much more than those for columns. This is due to the larger damage suffered by the beams compared to the columns, which is a consequence of the hierarchy of resistance imposed by the Eurocode 8 in the design for the high ductility class.

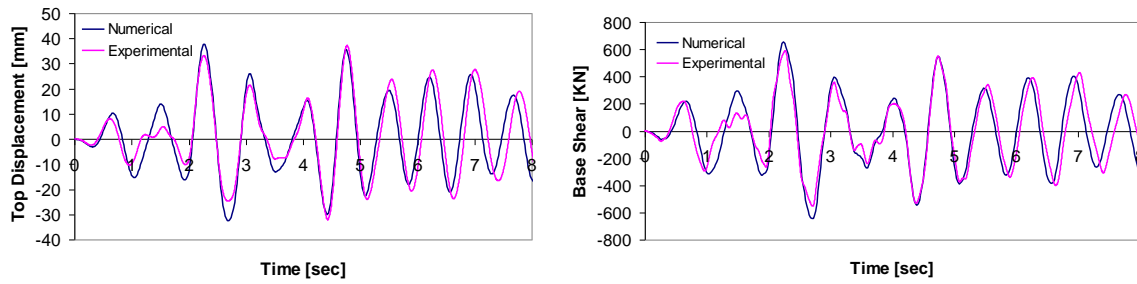


Figure 2. Top displacement and base shear time history response of the bare structure under low-level earthquake: experimental and numerical results

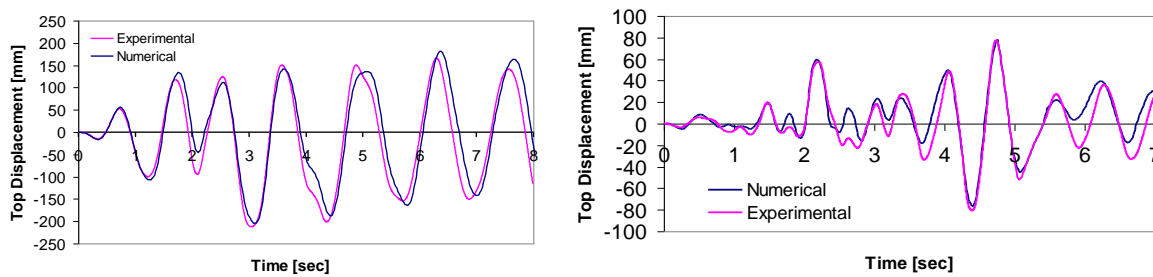


Figure 3. Top displacement time history response of the bare structure (left) and of the uniformly infilled structure (right) under high-level earthquake: experimental and numerical results

The accuracy of the models allowed to properly investigate the global and local response of the different structural configurations. One way of quantifying numerically the seismic damage suffered by buildings is by making use of damage indices. Among many damage indices proposed and available in literature, the Park & Ang damage index is widely used due to its relative simplicity and extensive calibration against experimentally observed seismic damage in reinforced concrete structures. The Park & Ang damage index, widely used to estimate damage in reinforced concrete ductile members, is a linear combination of the maximum ductility and the hysteretic energy dissipation demand imposed by the earthquake on the structure and is defined as, (Park and Ang, 1985):

$$DI = \frac{\mu_m}{\mu_u} + \beta \cdot \frac{E_h}{F_y \cdot \mu_u} \quad (2)$$

The parameter β characterizes the level of contribution of the dissipated hysteretic energy to the damage of the building. For well-detailed RC members, a typical value of $\beta=0.05$ is assumed. Figure 4 shows the damage distribution of the frame building in the two different configurations, when subjected to the high-level earthquake record, using the Park & Ang damage index. The uniform distribution of damage observed on the bare structure in the experimental tests was confirmed by the numerical analyses. The analysis of the maximum values of the damage index registered at the critical locations highlighted a weak beam-strong column mechanism, with a regular distribution of damage. The effects of the non-structural masonry infills placed at all stories of the external frames on the global seismic response of the structure were investigated. An increase in stiffness, strength and dissipation capacity was highlighted by numerical analyses. The regular distribution of infills resulted in a concentration of ductility demand at the lower stories. The column-to-beam damage index ratio was larger than in the case of the bare structure and the progressive formation of a storey-level

mechanism was observed. The progressive failure of the masonry infills at each storey may activate a series of weak-column strong-beam storey mechanisms, which may lead to high ductility demands in the columns. Smaller values of the damage index were registered at the upper stories with respect to the bare structure. The damage index values were in satisfactory agreement with the damage observed in the experimental tests. For well-detailed RC members, combined indices, such as Park & Ang, appear to be dominated by the monotonic ductility term, while energy plays only a marginal role and the energy dissipation doesn't affect the results significantly.

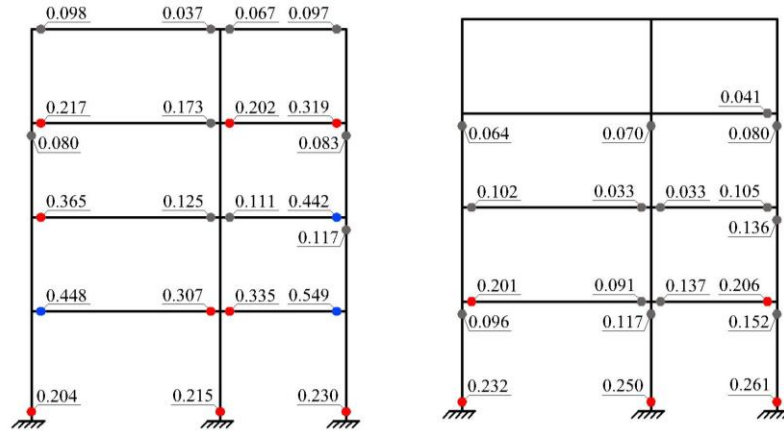


Figure 4. Damage distribution on the external frame of the R/C structure: bare (left) and infilled (right) configurations

4. Seismic performance assessment

According to Eurocode 8, a simplified assessment procedure based on nonlinear static analyses was adopted and the level of damage in the structures was evaluated with reference to three Limit States (LS): Damage Limitation (DL), Significant Damage (SD) and Near Collapse (NC). Each limit state is achieved in the structural model once a specific chord rotation is attained in one of the members of the structure: the LSDL, the LSSD and the LSNC correspond to the first attainment of θ_y , $0.75 \cdot \theta_u$ and θ_u , respectively. The deformation capacity of the structural members is evaluated in terms of chord rotation. An empirical conservative expression, implemented in Eurocode 8, was used for evaluating the member deformation capacity. The value of the total ultimate chord rotation capacity, θ_u , of concrete members under cyclic loading at the Limit State of Near Collapse was calculated from the following expression:

$$\theta_u = \frac{1}{\gamma_{el}} \cdot 0.016 \cdot 0.3^{\nu} \cdot \left[\frac{\max(0.01; \omega')}{\max(0.01; \omega)} \cdot f_c \right]^{0.225} \cdot \left(\frac{L_v}{h} \right)^{0.35} \cdot 25^{\left(\alpha \cdot \rho_{sa} \cdot \frac{f_{yt}}{f_c} \right)} \cdot (1.25^{100 \cdot \rho_d}) \quad (3)$$

The chord rotation θ_y at yielding was evaluated as:

$$\theta_y = \phi_y \cdot \frac{L_v}{3} + 0.0013 \cdot \left(1 + 1.5 \cdot \frac{h}{L_v} \right) + 0.13 \cdot \phi_y \cdot \frac{d_b \cdot f_y}{\sqrt{f_c}} \quad (4)$$

In Figure 5 the values of the chord rotation capacity for beams and columns are reported. The chord rotation capacity of columns was computed considering the axial load due to the gravity loads pertaining to the seismic combination. In the assessment procedure carried out in this study, the values of the chord rotation capacity were computed as a function of the seismic demand, considering the values of the axial load at each time step.

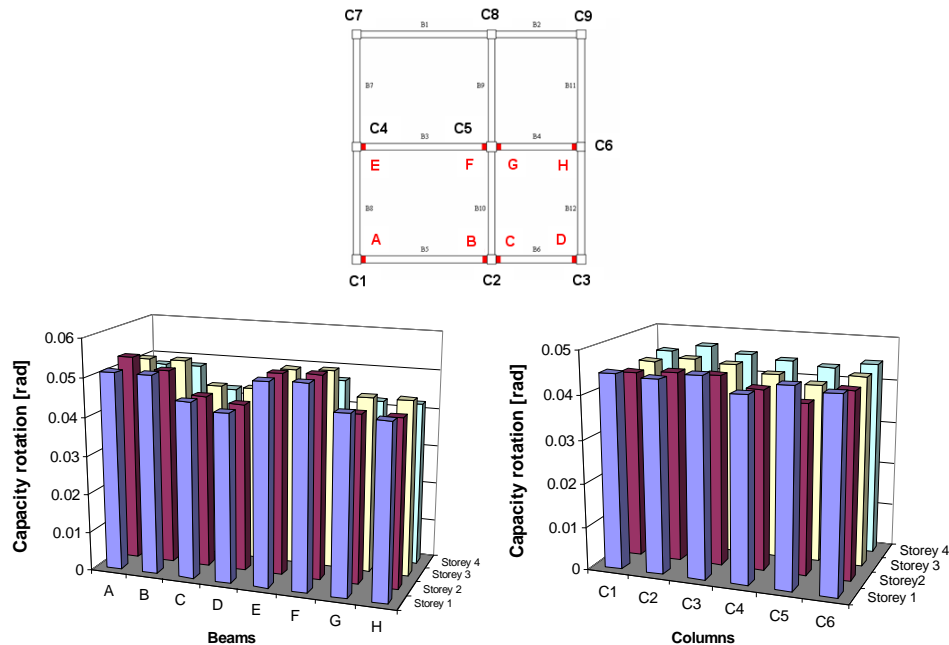


Figure 5. Chord rotation capacity of beams and columns of the bare structure subjected to gravity loads

Nonlinear static analyses were performed on the bare and masonry infilled structures. Two vertical distributions of the lateral loads were applied: a “uniform” pattern, based on lateral forces that are proportional to mass regardless of elevation and a “modal” pattern, proportional to lateral forces consistent with the lateral force distribution determined in elastic analysis. The base shear - top displacement curves obtained by push-over analyses using the “modal” pattern distribution are presented in Figures 6 - 8 for the bare and infilled structures.

The seismic demand was computed with reference to the Eurocode 8 response spectrum (Type 1, soil class B). The theoretical predictions were performed for a seismic intensity level equal to $S_{a_g}=0.4g$. Figure 6 shows that the bare structure was able to satisfy the seismic demand at the Limit State of Damage Limitation and Significant Damage, but lacked the appropriate capacity at the Limit States of Near Collapse. A gap in terms of maximum top displacement was observed at the LSNC and the difference between the seismic demand and the displacement capacity was 4.3 cm (34.6 cm vs 30.3 cm). The results of the simplified procedure showed that the first attainment of the member capacity occurred at the beam of the first floor, where the most significant damage was observed in the laboratory tests and the highest value of the Park & Ang damage index was registered during nonlinear dynamic analyses.

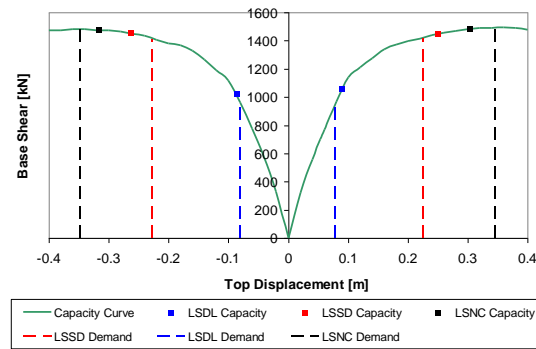


Figure 6. Displacement capacity and demand for the bare structure at the different limit states

Figure 7 shows that the structural capacity was greatly influenced by the presence of masonry infills. The expected contribution of the masonry infills in terms of both strength and stiffness was evident when comparing the response of the different frame configurations under monotonic loads. The maximum base shear of the infilled structure was much larger (1.7 times) than the bare structure. Masonry infills substantially increased the stiffness and strength of the structure. However, after a certain point the strength of the infilled structure substantially decreased with increasing deformations as a consequence of the progressive failure of infills, until it reached the strength of the bare structure. The higher stiffness provided by the masonry infills led to anticipate, in terms of drift, the development of global inelastic mechanisms in the infilled frames compared to the bare frame. A concentration of damage in the first storey of the infilled structure was observed.

The application of the simplified assessment procedure showed that the infilled structure was able to withstand the displacement demand due to seismic action equal to $Sa_g=0.4g$ for all the different limit states, Figure 7. At the LSNC the seismic demand in terms of top displacement was reduced to 10.8 cm, while the capacity of the structure was equal to 19.2 cm. The simplified assessment procedure showed that, if the contribution of the infill to the strength and stiffness of the structure was very large, the seismic demand was drastically reduced with respect to the bare structure. In the infilled structure an extensive damage in the masonry panel was registered at the first storey and the first attainment of the capacity of a member occurred at the column of the first floor.

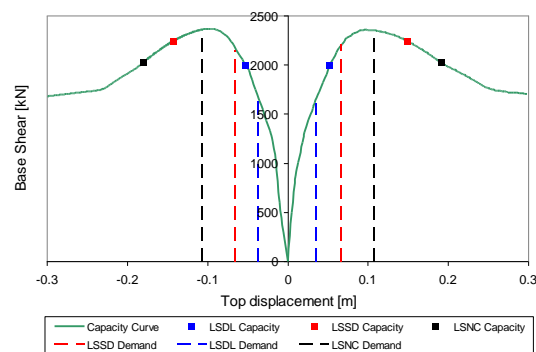


Figure 7. Displacement capacity and demand for the infilled structure at the different limit states

The influence of masonry openings on the response of the structure was investigated too. The presence of openings of different sizes was considered at each storey of the large bay of the structure. This paper presents some results obtained from numerical analyses on infill walls presenting 25% and

20% opening percentage, respectively, for the first and upper storeys, Figure 8. The equivalent diagonal strut model was used to represent the infill panel and openings were considered by varying the strut width. The introduction of openings affected the dynamic characteristics of the structure. As expected, the fundamental period increased with increasing the opening size due to reduction in stiffness of the model. The effects of openings on the behaviour of the structures were clearly evidenced by pushover analyses. The presence of openings within the infill walls decreased the stiffness and the strength of the uniformly infilled structure, and the drop of strength was less evident than the case of fully infilled structures, as shown comparing Figures 7 and 8. In case of infilled structure with openings the damage concentrated in the second storey. The application of the simplified assessment procedure showed that the infilled structure was able to withstand the displacement demand due to seismic action equal to $S_{a_g}=0.4g$ for all the different limit states.

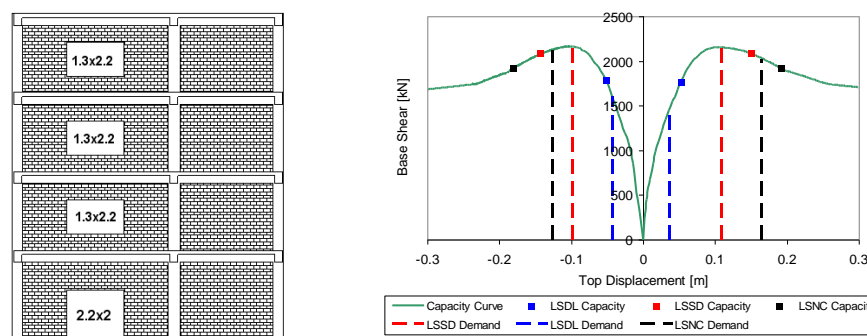


Figure 8. Elevation view of the infilled structure with openings (left) and displacement capacity and demand for the infilled structure with openings at the different limit states (right)

Nonlinear dynamic analyses were performed on the different structures under study by using seven scaled real accelerograms with satisfactory compatibility between the mean elastic response spectrum and the Eurocode 8 response spectrum (Type 1, soil class B). Different earthquake intensity levels were considered in the numerical analyses.

Figure 9 presents the maximum top displacements registered for the three structures for different seismic intensity levels (a_g ranges from 0.15g to 0.6g). A considerable reduction of the maximum top displacements was observed in case of structures with masonry infills compared with the bare structure. The top displacement of the infilled structure increased with the presence of openings and with the increase of opening sizes as the structures became more flexible.

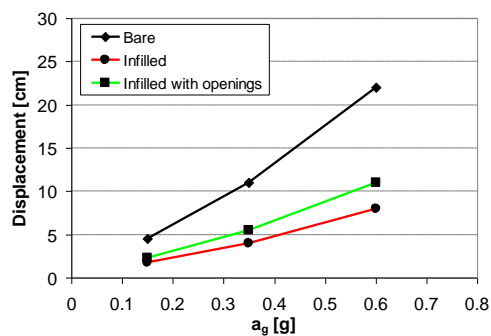


Figure 9. Maximum top displacements of the structures under study for different seismic intensity levels

Figure 10 shows the inter-storey drift profiles along the height of the analyzed structures under seismic intensity level equal to 0.6g and the influence of the masonry infills on the structural behaviour was apparent. The inter-storey drift profiles indicate that the distribution of damage is different between the bare and infilled structures. The maximum drift demand on the bare structure was registered at the second storey. On the contrary, the drift demands on the uniformly infilled structure concentrated at the first storey without any excessive demands at the upper storeys.

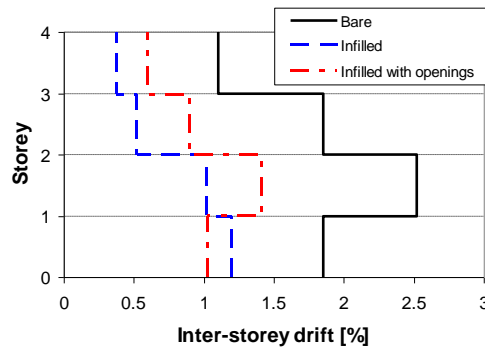


Figure 10. Inter-storey drift profiles for the investigated structures under accelerograms with $a_g=0.6g$

As expected, numerical analyses showed an increase of both strength and stiffness for the infilled structures with respect to the bare counterpart. The masonry infills caused a significant increase of the maximum base shear, as presented in Figure 11. The increment of the base shear was influenced by the masonry openings, which reduced the maximum values for the infilled structures. Satisfactory agreement in terms of base shear values was observed comparing numerical results of the pushover and time-history analyses. The column contribution to storey shear in the infilled structure without openings resulted lower than in the bare structure. In presence of masonry openings, the column contribution to storey shear increased.

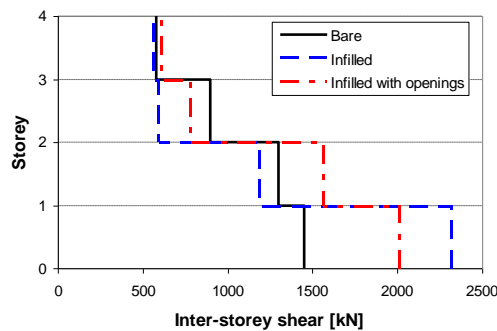


Figure 11. Inter-storey shear profiles for the investigated structures under accelerograms with $a_g=0.6g$

5. Different types of infills

The influence of the mechanical properties of the infill panels on the response of the structure was investigated considering different types of infills. The mechanical properties of the infills assigned to

the numerical model were derived according to practice. Two variants of masonry infills, aimed at simulating weak and strong infill panels, were investigated and different models were generated. Autoclaved aerated concrete (AAC) infill walls were also considered in the numerical analyses. Nonlinear static analyses were performed on the infilled models and the base shear - top displacement curves are presented in Figures 12 - 14 for different infill panels. The structural capacity of the models was greatly influenced by the different types of infill panels. Strong masonry infills substantially increased the stiffness and strength of the structure, Figure 12. However, a considerable reduction of strength occurred after the failure of the infill at the first storey. The strength degradation was less marked in presence of AAC walls and weak masonry, Figures 13 and 14.

The application of the simplified assessment procedure showed that the strong masonry infilled model and the model with AAC infill walls were able to withstand the displacement demand due to seismic action with peak ground acceleration $Sa_g=0.4g$ for all the different limit states, Figures 12 and 13. On the contrary, the weak masonry infilled model was unable to satisfy the seismic demand at the Limit States of Near Collapse, Figure 14.

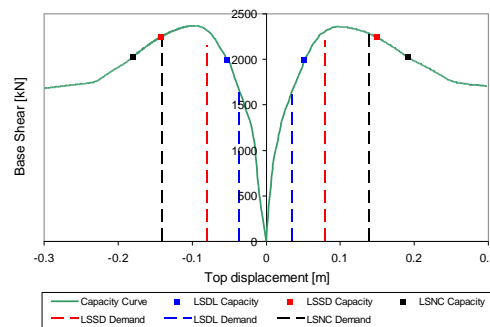


Figure 12. Displacement capacity and demand for the strong masonry infilled structure at the different limit states

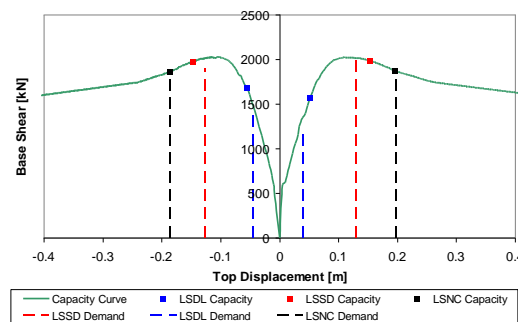


Figure 13. Displacement capacity and demand for the AAC infilled structure at the different limit states

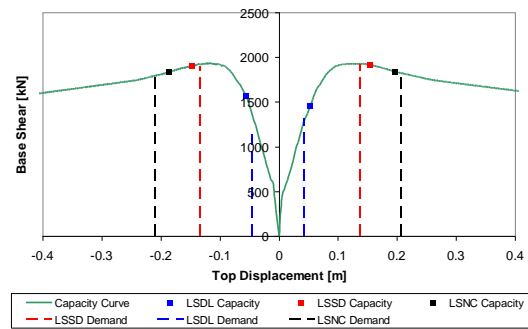


Figure 14. Displacement capacity and demand for the weak masonry infilled structure at the different limit states

Nonlinear dynamic analyses under accelerograms with intensity level equal to 0.6g were performed on the infilled structures and the inter-storey drift profiles along the height of the structures are reported in Figure 15. The different types of infills changed the distribution of damage throughout the structure. The maximum drift demand on the weak masonry infilled model was registered at the second storey. On the contrary, the drift demands on the strong masonry infilled model concentrated in the first two storeys. This different behaviour was more evident under high levels of ground motion intensity.

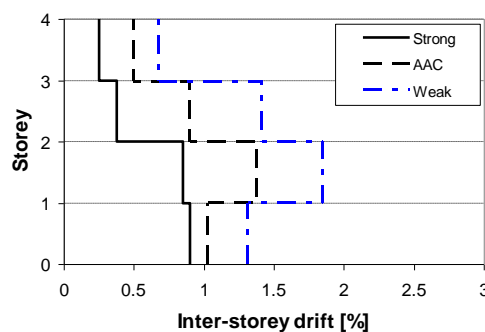


Figure 15. Inter-storey drift for the infilled structures under accelerograms with $a_g=0.6g$

6. Conclusions

The seismic performance of a ductile R/C structure with masonry infills was studied by nonlinear static and dynamic analyses and the effects of infills on the structural response were investigated. The expected contribution of the masonry infills in terms of both strength and stiffness was evident when comparing the response of the different structural configurations under nonlinear static analyses. The increase of stiffness provided by the masonry infills led to anticipate, in terms of drift, the attainment of the different Limit States in the infilled structure with respect to the bare counterpart. The presence of uniformly distributed infills considerably changed the distribution of damage throughout the structure. The maximum drift demand on the bare structure was registered at the second storey. On the contrary, the drift demands on the uniformly infilled structure concentrated at the first storey without any excessive demands at the upper storeys. The sudden reduction of strength due to the damage of the infills can lead to severe damage for severe seismic input motions. For the infilled structures, the deformation capacity at the LSNC was large enough to accommodate the demand and a

significant reduction of the damage was registered compared to the bare structure. The influence of uniformly distributed infills on the seismic response of the investigated structure was beneficial according to the simplified assessment procedure. The presence of masonry openings and the mechanical properties of the infills affected the distribution of damage throughout the structure. Two variants of masonry infills aimed at simulating weak and strong infill panels were investigated. Strong masonry infills significantly contributed to the lateral stiffness and load resistance of the structure, but a sudden decrease of strength was observed after the failure of infills.

References

- Asteris P.G. (2003). Lateral stiffness of brick masonry infilled plane frames. *Journal of Structural Engineering*, 129(8), 1071-1079.
- Carr A.J. (2006). Ruaumoko Program for Inelastic Dynamic Analysis. Department of Civil Engineering, University of Canterbury, Christchurch, New Zealand.
- CEN (2004) European Standard EN 1998-1. Eurocode 8: Design of structures for earthquake resistance. Part 1: General rules, seismic action and rules for buildings. European Committee for Standardization, Brussels.
- CEN (2005) European Standard EN 1998-3. Eurocode 8: Design of structures for earthquake resistance. Part 3: Assessment and retrofitting of buildings. European Committee for Standardization, Brussels.
- Crisafulli F.J., (1997). Seismic Behaviour of Reinforced Concrete Structures with Masonry Infills. PhD Thesis, Department of Civil Engineering, University of Canterbury, Christchurch, New Zealand.
- Crisafulli F.J., Carr A.J., Park R. (2000). Analytical modelling of infilled frame structures – A general overview. *Bulletin of the New Zealand Society for Earthquake Engineering*, 33(1), 30-47.
- Mander J.B., Priestley M.J.N., Park R., (1988). Theoretical Stress-Strain Model for Confined Concrete. *Journal of Structural Engineering*, 114(8), 1804-1826.
- Martinez-Rueda J.E., Elnashai A.S., (1997). Confined concrete model under cyclic load. *Materials and Structures*, 30(197), 139-147.
- Menegotto M., Pinto P.E., (1973). Method of analysis for cyclically loaded R.C. plane frames including changes in geometry and non-elastic behavior of elements under combined normal force and bending. Preliminary Report, IABSE, Zurich, 13, 15-22.
- Negro P., Verzeletti G., Magonette G.E., Pinto A.V., (1994). Tests on a four-story full-scale R/C frame designed according to Eurocodes 8 and 2: Preliminary Report. Report EUR 15879 EN, European Commission, Joint Research Centre, Ispra, Italy.
- Negro P., Anthoine A., Combescure D., Magonette G.E., Molina J., Pegon P., Verzeletti G., (1995). Test on a four-storey full-scale reinforced concrete frame with masonry infills: Preliminary Report. Special publication No. I.95.54, European Commission, Joint Research Centre, Ispra, Italy.
- Otani S., (1974). Sake, A Computer Program for Inelastic Response of R/C Frames to Earthquakes. Report UILU-ENG-74-2029, Civil Engineering Studies, University of Illinois at Urbana-Champaign.
- Paulay T., Priestley M. J. N., (1992). Seismic design of reinforced and masonry buildings. John Wiley & Sons.

Park Y.J., Ang A.H.S., (1985). Mechanistic seismic damage model for reinforced concrete. *Journal of Structural Engineering*, ASCE, 111: 722–739.

SeismoSoft (2007). *SeismoStruct – A Computer Program for Static and Dynamic Nonlinear Analysis of Framed Structures*.